Ultraviolet photoelectron spectroscopic study of boron adsorption and surface segregation on Si(111)

J. Krügener,[1] H. J. Osten,[2] and A. Fissel[1]

[1]*Information Technology Laboratory, Leibniz Universität Hannover, Schneiderberg 32, D-30167 Hannover, Germany*

[2]*Institute of Electronic Materials and Devices, Leibniz Universität Hannover, Schneiderberg 32, D-30167 Hannover, Germany*

(Received 1 July 2010; revised manuscript received 22 December 2010; published 3 May 2011)

The adsorption and surface segregation behavior of elemental boron (B) deposited on Si(111) have been studied by ultraviolet photoelectron spectroscopy and accompanying reflection high-energy electron diffraction as a function of the B coverage (c_B) and annealing temperature (T). Our results clearly demonstrate an effective incorporation of B into subsurface sites at $T > 800$ K and formation of a well-ordered $(\sqrt{3} \times \sqrt{3})R30^\circ$ surface superstructure. Thereby, a critical c_B of about 0.6 monolayers (ML) was determined for different conditions to prevent surface defects resulting from Si dangling bonds, which appear as surface states at 0.4 eV below the Fermi level. Annealing of the defect-free $(\sqrt{3} \times \sqrt{3})R30^\circ$ superstructure covered by several MLs Si at $T \geqslant 1040$ K results in a renewal of the perfect B-induced Si surface structure, even after several deposition and annealing cycles. This indicates a dominance of B surface segregation over bulk diffusion. Significant B bulk diffusion commences only above 1100 K. Differences were found for spectra obtained for the B-induced surface structures formed after deposition and surface segregation, respectively. An additional surface state appeared at 2.1 eV below the Fermi level after deposition of 0.6 ML B. The state could be attributed to boron-boron interaction due to the presence of small clusters at the surface. This surface state did not disappear after high-T annealing and was not observed for lower c_B and after B surface segregation, respectively.

DOI: 10.1103/PhysRevB.83.205303 PACS number(s): 81.15.Hi, 68.35.B−, 79.60.−i, 61.05.jh

I. INTRODUCTION

For novel device architectures, crystal structure engineering instead of the commonly used material engineering might be a future solution.[1–4] In particular, different silicon structures (Si polytypes) are recommended for sophisticated devices.[5–9] Problems due to different chemical constituents, e.g., in commonly used silicon-germanium heterobipolar transistors,[10] can be avoided in that way. Furthermore, the heterostructure interfaces should be inherently defect-free, lattice matched, and coherent. As reported in several growth experiments, epitaxial growth of Si on boron- (B-) covered Si(111) surface results in a change of Si epitaxial layer orientation under certain conditions.[9,11,12] For that purpose, epitaxial growth of Si on B-covered Si(111) has become an interesting research object recently[9,12,13] and some attempts have been made to prepare artificially stacked Si structures, such as twinning superlattices, by periodical variation of the molecular beam epitaxy (MBE) growth conditions.[9,12]

During the deposition of B on Si(111), the surface structure transforms from (7×7) for a well-prepared surface to a $(\sqrt{3} \times \sqrt{3})R30^\circ$ surface superstructure, which is completed at 1/3 monolayer (ML) of B coverage (c_B).[14] Here, 1 ML is defined as the surface atom density of the truncated Si(111)(1×1) surface. Initially, the $(\sqrt{3} \times \sqrt{3})R30^\circ$ superstructure was assumed to be formed by B atoms occupying T_4 adatom positions at the surface. After high-temperature (T) annealing, the structure of the $(\sqrt{3} \times \sqrt{3})R30^\circ$-B surface consists of B atoms in fivefold-coordinated substitutional S_5 sites directly under Si adatoms occupying T_4 positions.[15–17] In that case, the surface contains only Si adatoms without dangling bonds, due to a charge transfer from the Si atoms in T_4 sites to the B atoms in S_5 sites. This should also have some influence on the further epitaxial growth of Si.

Indeed, the growth mode on $(\sqrt{3} \times \sqrt{3})R30^\circ$-B changes under certain conditions to a two-bilayer (2BL) growth mode,[13,18,19] whereas the growth on the (7×7) reconstructed Si(111) is governed by a BL growth mode. Thus, the 2BL islands nucleate in twin orientation with respect to the substrate.[12]

Up to now, the growth of homogeneous artificially stacked Si layers is restricted to small areas across a substrate.[9] It was suggested that this is mainly caused by an inhomogeneous growth process.[13] There it was shown that the growth mode on B-covered Si(111) strongly depends on the amount of B present at the surface. In reflection high-energy electron diffraction (RHEED) intensity studies, a transient growth behavior with irregular intensity oscillations was observed for c_B in the range of $0.2 \leqslant c_B < 0.5$ ML (Fig. 1, left side). The observed behavior was suggested to be associated with surface defects of an imperfect $(\sqrt{3} \times \sqrt{3})R30^\circ$ surface structure, which was verified very recently by ultraviolet photoelectron spectroscopy (UPS) studies.[20] Si dangling bonds appearing in case of insufficient c_B were identified as the main defects, resulting in a surface state (A_1, Fig. 1, center) with an energy slightly below the Fermi level (−0.4 eV). The appearance of the surface state was found to be accompanied by a significant Fermi level pinning which is typical for surface dangling bond states (Fig. 1, center and right side). A critical coverage of $c_B > 0.5$ ML has been determined to prevent this kind of surface defect (Fig. 1, middle).

To realize Si nucleation in a certain configuration homogeneous at least within large areas across the substrate, the surface structure should be perfect. That demands detailed understanding of surface structure formation and defect engineering. In this context, several points are still not fully understood with respect to the B-induced $(\sqrt{3} \times \sqrt{3})R30^\circ$-B structure and it is an intention of this work to illuminate some of the critical issues:

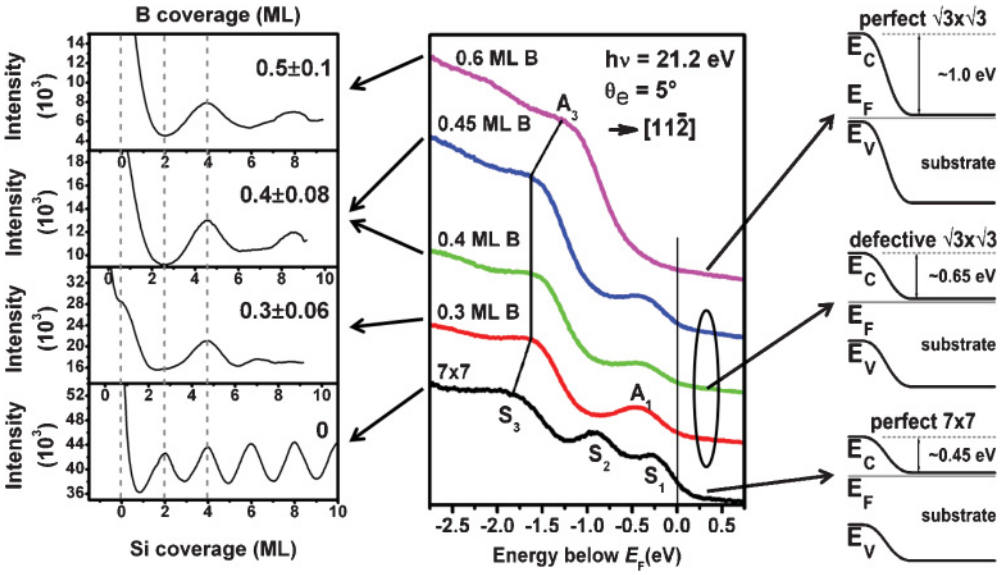

FIG. 1. (Color online) RHEED intensity studies as a function of B coverage showing a gradual transition from BL to 2BL growth for $0 \leqslant c_B \leqslant 0.5$ ML (left). This behavior is suggested to be associated with surface defects of an imperfect surface structure. UPS studies show the occurrence of a surface defect (A_1) for $c_B < 0.6$ ML (middle). The presence of the defect state is accompanied by a significant Fermi level pinning. Band bending diagram for (7 × 7), defective ($\sqrt{3} \times \sqrt{3}$), and perfect ($\sqrt{3} \times \sqrt{3}$) on *n*-type Si(111) is also shown (right side).

(a) the characteristics in terms of the $(\sqrt{3} \times \sqrt{3})R30°$-B surface structure formation by deposition and segregation of B,

(b) the critical c_B for the formation of defect-free surface structures as a function of the preparation conditions, such as substrate T during B deposition, and T and duration of subsequent annealing, and

(c) the critical conditions (T and duration) for the formation of defect-free surface structures by surface segregation of buried B after Si growth.

In the literature, only a few reports can be found dealing with surface electronic structure of Si(111)$(\sqrt{3} \times \sqrt{3})R30°$-B prepared by B deposition.[17,20–22] In view of these few investigations, it is not clear whether or not the Si(111) surface structure depends on the source material used for B deposition. Moreover, comparative studies of the electronic structure of Si(111)$(\sqrt{3} \times \sqrt{3})R30°$ surfaces prepared by B deposition and surface segregation cannot be found in literature (to the best of the authors knowledge). Therefore, it is also an intention of this study to provide further insight into the surface structure of Si(111) induced by elemental B.

In this paper, we report on detailed UPS investigations of the B-induced $(\sqrt{3} \times \sqrt{3})R30°$ surface structure formation as a function of T during elemental B deposition and annealing and also as a function of annealing duration in order to estimate the critical conditions for preparation of perfect $(\sqrt{3} \times \sqrt{3})R30°$ surface structure. Further, the successive evolution of the surface electronic structure of Si(111) by segregation of buried B has also been studied as function of time and T. This was also be done in order to check whether or not the initial c_B is high enough for the renewal of a perfect $(\sqrt{3} \times \sqrt{3})R30°$ structure by surface segregation. This is of practical importance with respect to the realization of artificial structures, since otherwise the c_B always has to be increased after each Si growth. The segregation behavior was also studied with respect to multistructures. For this purpose, several deposition/annealing cycles, as described in Fig. 2, were performed by varying the annealing T and duration, respectively. In addition, RHEED measurements were performed to monitor the surface reconstruction during all process steps. Based on that, optimized conditions have been established for the preparation of a defect-free B-induced Si(111)$(\sqrt{3} \times \sqrt{3})R30°$ surface structure during the different steps for the epitaxial growth of an artificially stacked Si structure.

II. EXPERIMENT

Si layers were grown by solid-source MBE on 4-in. *n*-type Si(111) (phosphorus doped, 10^{17} cm^{-3}) wafers with a miscut of $\leqslant 0.1°$. The substrates were prepared *ex situ* by standard wet-chemical RCA (Radio Corporation of America) cleaning, ultraviolet-ozone plasma treatment, and a subsequent etching in dilute HF. *In situ*, the substrates were prepared further by a treatment at $T = 1000$ K under a slight Si flux, where Si was evaporated by electron beam heating with a rate of about 1 nm/min. The same rate was used to grow the Si layers in the experiments, where the Si rate was determined by measuring RHEED specular beam intensity oscillations.[13,20] After this treatment, the Si(111) surface exhibited a well-developed (7×7) reconstruction. The substrate T was measured by a thermocouple just behind the sample holder, calibrated by an optical pyrometer. The real T of the substrate surface was checked additionally using the (7×7)-(1×1) surface phase transition which occurs around 1100 K.[23,24] B was evaporated from an effusion cell at $T > 2000$ K, corresponding to a deposition rate of around 0.02 ML/min. RHEED intensity measurements of certain surface superstructure spots were used to determine c_B during

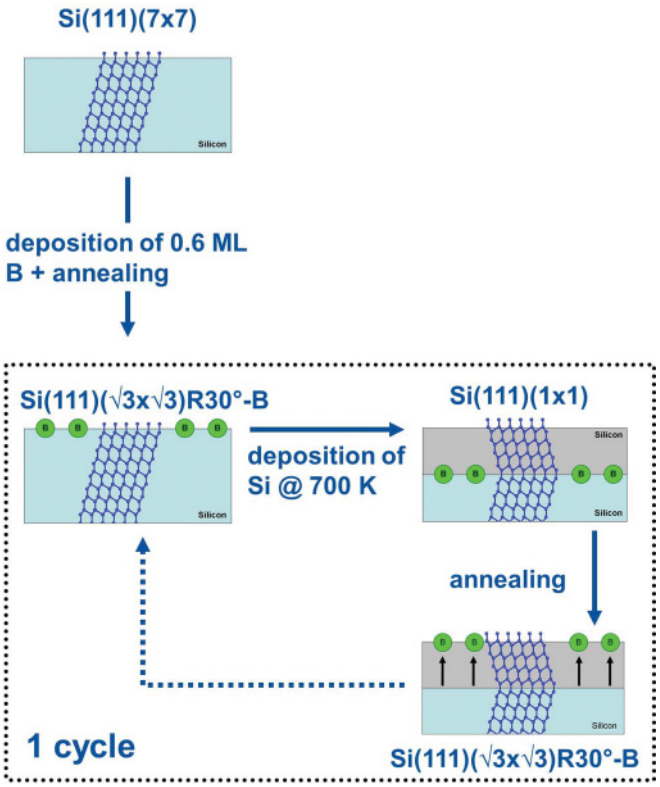

FIG. 2. (Color online) Flowchart of Si deposition/annealing cycles used for surface preparation in surface segregation studies.

formation of the Si(111)$(\sqrt{3}\times\sqrt{3})R30°$-B surface superstructure, as described elsewhere.[13,20] UPS measurements were conducted in the same multichamber vacuum system at a working pressure of 2×10^{-8} torr using a He discharge source (Specs 10/35), with unpolarized light of 21.2 eV photon energy (He I_α). The photoemitted electrons were analyzed with a hemispherical analyzer (Thermo-VG100AX) using step sizes of 10 meV and a pass energy of 8.5 eV. The emission angle (θ_e) was fixed at 5° with respect to the surface normal (point P in Fig. 3) with an angular resolution of 0.1°. The photon incidence angle θ_i was fixed in the plane perpendicular to the azimuthal angle of emission, which was chosen in the [11$\bar{2}$] direction. The samples were biased negatively (−12 V), to prevent a floating potential. In the measurements the bias voltage appears as a simple offset in the UPS spectra. The stability of the voltage has been checked to be ±0.05 eV by repeating measurements on the same area of the same sample within a period of some days. The electron binding energy was calibrated relative to the positions of the S_1 and S_2 surface states of the initial (7×7) surface structure since they are well investigated and do not show significant dispersion.[25]

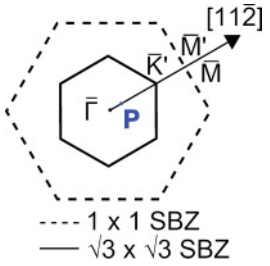

FIG. 3. (Color online) Geometry of the (1×1) and $(\sqrt{3}\times\sqrt{3})R30°$ surface Brillouin zone (SBZ) of the Si(111) surface. The point marked P in the [11$\bar{2}$] direction corresponds to the emission angle of 5° used for the UPS studies.

III. RESULTS AND DISCUSSION

A. UPS study of the surface electronic structure of Si(111) during boron deposition and subsequent annealing

UPS spectra obtained for Si(111)$(\sqrt{3}\times\sqrt{3})R30°$-B surfaces prepared by deposition of 0.6 ML B at 810 and 860 K, respectively, are shown in Fig. 4. For comparison, the spectrum obtained for the Si(111)(7×7) surface is also shown, where the three surface states at −0.25 eV (S_1, adatom dangling-bond state), −0.9 eV (S_2, rest atom state), and at −1.8 eV (S_3, back bond state) are indicated. The peaks visible around −4.5 and −7.5 eV correspond to emission from Si bulk states (3p,3sp).[26,27] Further experiments were conducted with respect to the surface structure development during subsequent annealing for samples prepared by deposition of 0.6 ML B at 860 K. Figure 5 shows spectra obtained after subsequent annealing of these samples at T between 1000 and 1130 K for a duration of 10 min.

In comparison to Si(111)(7×7), the UPS spectra for the B-covered surface only exhibit two states near the Fermi level, labeled as A_3 and A_4. No peak is visible around −0.4 eV indicating absence of Si dangling bonds. The state at −1.2 eV (A_3) is related to emission from the back bonds as already shown in earlier investigations.[28] We suggest that the peak appearing around −2.1 eV (A_4) is already an indication for the

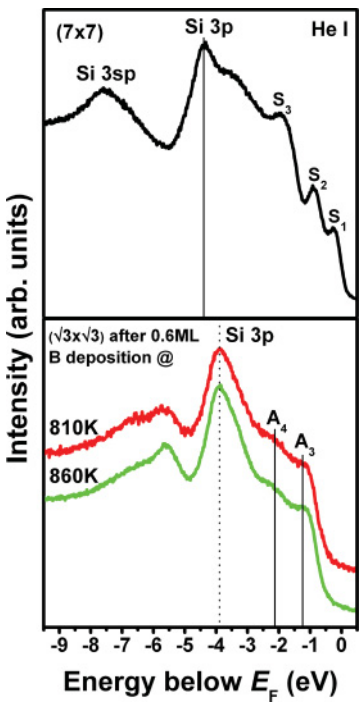

FIG. 4. (Color online) UPS spectra for Si(111)$(\sqrt{3}\times\sqrt{3})R30°$-B surface, where 0.6 ML B was deposited at 810 and 860 K, respectively. The topmost curve shows an UPS spectrum of the initial Si(111)(7×7) surface structure.

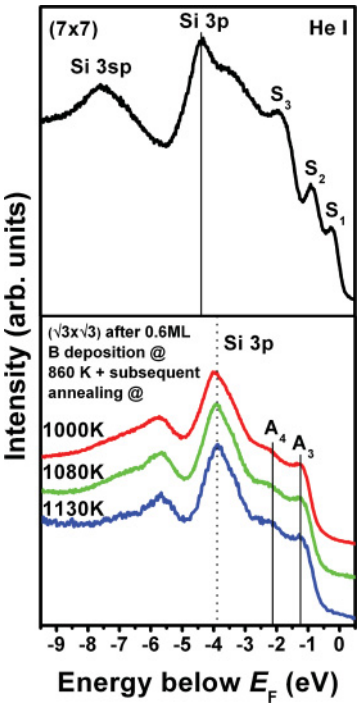

FIG. 5. (Color online) UPS spectra for Si(111)$(\sqrt{3}\times\sqrt{3})R30^\circ$-B surface, where 0.6 ML B was deposited at 860 K and subsequently annealed at different T for a duration of 10 min. The topmost curve shows an UPS spectrum of the initial Si(111)(7×7) surface structure.

specific surface structure induced by elemental B, which will be discussed later. The support for this hypothesis is obtained from further studies presented in the next section.

In the low-energy range of the spectra, the Si bulk state (3p) is much sharper and more intense than for the clean (7×7) surface and is shifted by about 0.5 eV with respect to (7×7). The peak sharpening indicates a more bulklike atomic order for the Si(111)$(\sqrt{3}\times\sqrt{3})R30^\circ$-B sample in the near-surface region probed by UPS, as suggested for example for the Si(111)(1×1) surface induced by As.[29] In the low-energy range, there is also visible a peak centered at −5.8 eV with a shoulder toward the lower-energy side. Whereas the shoulder can be associated with emission from Si bulk states (3sp), the nature of the peak at −5.8 eV is still unclear at this point and will also be discussed later.

The samples prepared in different ways exhibited a well-developed Si(111)$(\sqrt{3}\times\sqrt{3})R30^\circ$-B surface structure in RHEED (not shown here) and the corresponding UPS spectra do not show differences. That is surprising since within the investigated range of T a B site exchange from T_4 to S_5 should occur as suggested by other groups.[21,30] For example, a range of $T \geqslant 1073$ K was assumed for the site exchange based on core level X-ray photoelectron spectroscopy (XPS) measurements[21] and work function measurements in combination with scanning tunneling microscopy (STM) investigations.[31] On the one hand, this may indicate that the UPS spectra are not affected by site exchange under the conditions used in our case (direction of photon incidence and detection angle).

On the other hand, the published results with respect to the side exchange are for Si(111)$(\sqrt{3}\times\sqrt{3})R30^\circ$-B surfaces prepared in different ways. In earlier STM and spectroscopic studies, for example, the Si(111)(7×7) was exposed to decaborane (DB) ($B_{10}H_{14}$) at room T and subsequently annealed at $T > 770$ K for hydrogen desorption. Even after deposition of DB at 900 K, only disordered surface structures were observed.[32] In contrast, our RHEED pattern of the Si(111) surfaces obtained by deposition of elemental B at the same T correspond to a well-ordered $(\sqrt{3}\times\sqrt{3})R30^\circ$ surface structure.

Therefore, we suggest that B occupies mainly S_5 sites in our studies even at lower T. Since the B-Si bond is short compared to Si-Si, occupation of T_4 sites by B results in a high strain within the surface and it is questionable therefore that B really will stay on T_4 sites at medium T. Instead, we presume that most of the B occupies the subsurface sites during the transformation of the complex (7×7) into the B-induced $(\sqrt{3}\times\sqrt{3})$ surface structure already at medium T of about 800 K. This is supported by the observed high-energy shift of the UPS spectra with respect to (7×7), indicating an effective doping due to the incorporation of B into substitutional sites in subsurface regions, as discussed recently.[20] But, since the c_B was higher than 1/3 ML necessary to form a perfect $(\sqrt{3}\times\sqrt{3})$, it cannot be excluded that additional B is also occupying other surface sites or may form clusters.

Recently, Stimpel *et al.* also used elemental B to prepare the B-induced surface superstructure.[31] Based on work function measurements, they suggested that B occupies the S_5 sites only at $T > 1100$ K. Unfortunately, they did not make any spectroscopic study to verify that suggestion. In STM studies they observed the successive substitution of Si adatoms by B during deposition at 900 K, where the $(\sqrt{3}\times\sqrt{3})$ reconstruction was found to be completed as soon as 45% of the surface consists of B atoms. Deposition of extra B results in the formation of amorphous B clusters, which disappeared after high-T annealing ($T > 1100$ K).

In view of similar preparation conditions used in our experiments, we suggest that the appearance of the surface state at 2.1 eV below the Fermi level can be attributed to excess B. This hypothesis is supported by the fact that such a peak was not observed at $c_B < 0.5$ ML in our previous studies.[20]

To clarify this point and, moreover, to get information as to which peaks are related to emission from B bulk states, UPS studies were performed for Si(111) surfaces with B deposited at lower T and higher coverage, respectively. In this case 0.6 and 1.3 ML B, respectively, were deposited at 670 K on Si(111)(7×7) surfaces. Subsequently the samples were annealed at 1130 K for 10 min. Accompanying surface structure investigations were made by RHEED to study the surface structure evolution during B deposition at low T.

In Fig. 6 are shown the obtained UPS spectra for the differently prepared Si(111) surfaces. The spectra for low T are clearly different from those obtained for deposition at higher T and exhibit three characteristic emission bands. The first band extends from about −0.5 to −5 eV with a shoulder at around −1.3 eV and a peak at around −4 eV. A second band is centered at around −6.5 eV and a third band extends from around −9 eV to the secondary electron (SE) peak at around −16 eV. For 1.3 ML, there is further seen an intensity shoulder at around −13 eV and a small peak at around −10 eV, whereas two small peaks at around −11.5 and −13 eV appeared for 0.6 ML B.

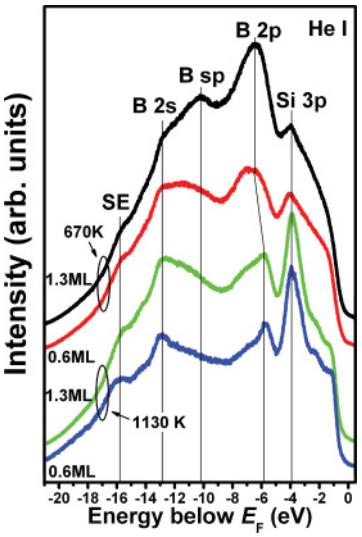

FIG. 6. (Color online) UPS spectra for Si(111) surface, where 0.6 and 1.3 ML B, respectively, were deposited at 670 K (two topmost curves). UPS spectra obtained after annealing at 1130 K for 10 min for initial $c_B = 0.6$ and 1.3 ML, respectively (two lowermost curves).

The intensity of the band around −6.5 eV increases for higher c_B. This is accompanied by an increase in intensity of the third band around −10 eV. Comparing our results with those obtained for DB on Si(111),[33] for DB on Mo(100),[34] and for iron borides,[35] we suggest that the broad band around −6.5 eV results from B 2*p* emission. Furthermore, the peak at around −13 eV likely originates from B 2*s* emission, whereas the peak observed at −10 eV for 1.3 ML B could arise from B *sp* hybridization. The appearance of B *sp* states is likely due to the presence of bigger amorphous B clusters. The intensity of the peak appearing in our investigations at around −4 eV does not change with c_B. We suggest that this peak is mainly associated with emission from Si bulk states superimposed by B-related emission.

In view of our obtained spectra, we can assume that B at low T is mainly at the surface and has formed clusters, which would compare to the results obtained by Stimpel *et al.* for $T = 900$ K.[31] We suggest that the formation of hybridized B clusters is favored over superstructure formation at low T and higher c_B.

Subsequent annealing of the samples for 10 min at 1130 K results in a drastic change of the spectra, which become comparable to spectra shown earlier in this section. There is seen a drastic intensity drop of the band around −6.5 eV, especially for 1.3 ML B. That compares to earlier studies for the high-T annealing of 1.1 ML B on Mo(100),[34] where it was suggested that B is incorporated below the surface during high-T annealing. In our spectra only a small band with a peak shifted to −5.8 eV and a shoulder to the low-energy side remained. Therefore, the peak at −5.8 eV can be attributed to emission from 2*p* states of B mainly incorporated into the subsurface regions, but shifted to lower binding energy due to the charge transfer from Si to B. The shoulder results from Si bulk emission.

Furthermore, the peak around −10 eV (B *sp*) vanishes, indicating the dissolution of larger B clusters. The peak at −13 eV associated with 2*p* emission is still visible after annealing.

In the high-energy range, the intensity of the peak located at −4 eV becomes more strongly visible and from the intensity between −4 and −1.3 eV only the peak at around −2.1 eV remains. Therefore, the suggestion that this peak is associated with remaining B at the surface after high-T annealing, such as within smaller clusters, is justified. This may have to do with the fact that in our case an elemental solid source is used for B evaporation. In that case a large variety of three-dimensional B clusters already exist within the B flux.[36] On the other hand, already in the solid state, B tends to cluster at high concentrations with a certain size and structure.[37–40] The same can be expected on surfaces in case of B excess. There could be two reasons for the presence of B clusters at the surface, self-assembling or direct adsorption of stable B clusters. In the case of direct adsorption, however, the peak at −2.1 eV should appear after high-T treatment also at lower c_B. Since this was not the case, the direct adsorption of stable B clusters can be excluded. Furthermore, direct adsorption would lead to the presence of three-dimensional clusters, which are less stable at the surface than two-dimensional clusters. We can therefore suggest that under conditions of B excess and high-T annealing mainly two-dimensional clusters are formed in a self-assembling way. Thus, the stability of these clusters is determined by their size and structure. For example, an unusual stability of planar and quasiplanar B_{12} clusters has recently been established.[41]

Furthermore, free B clusters were characterized using photoelectron spectroscopy and *ab initio* calculations.[42] An electronic state at 2.2 eV below the Fermi level was found for the planar anionic B_{12}^--cluster, which is close to the state observed in our study. Furthermore, the band formed between −4 and −1 eV after B deposition at low T may be associated with different bonding states of surface B. A large variety of states associated with surface B or B clusters have been reported located within this energy range.[42–46] Despite the strong evidence of B cluster formation, further work is needed to clarify the nature of the state appearing at −2.1 eV in our study.

The agglomeration of B into bigger clusters at low T with no long-range ordering is supported by the observed RHEED patterns (Fig. 7). After deposition of 0.6 ML B at 670 K, the RHEED pattern show a superposition of (7×7) and $(\sqrt{3} \times \sqrt{3})$ [Fig. 7(b)]. Increasing the c_B to 1.3 ML results in a decrease of the (7×7)/$(\sqrt{3} \times \sqrt{3})$ spot intensity ratio, which is due to more extended $(\sqrt{3} \times \sqrt{3})$ areas and smaller (7×7) areas [Fig. 7(d)]. This is consistent with results of earlier STM investigations,[17] where it was shown that the formation of the $(\sqrt{3} \times \sqrt{3})R30°$-B superstructure on Si(111)(7×7) needs larger amounts of B for lower T. Together with our recent RHEED studies,[13,20] the observed RHEED patterns allow us to estimate the amount of B involved in the $(\sqrt{3} \times \sqrt{3})$ superstructure formation to be approximately 0.15 and 0.25 ML for a total c_B of 0.6 and 1.3 ML, respectively.

B. Influence of annealing duration on the boron-induced surface electronic structure of Si(111)

Because the exchange demands thermal activation, the formation of a perfect Si(111)$(\sqrt{3} \times \sqrt{3})R30°$ surface structure

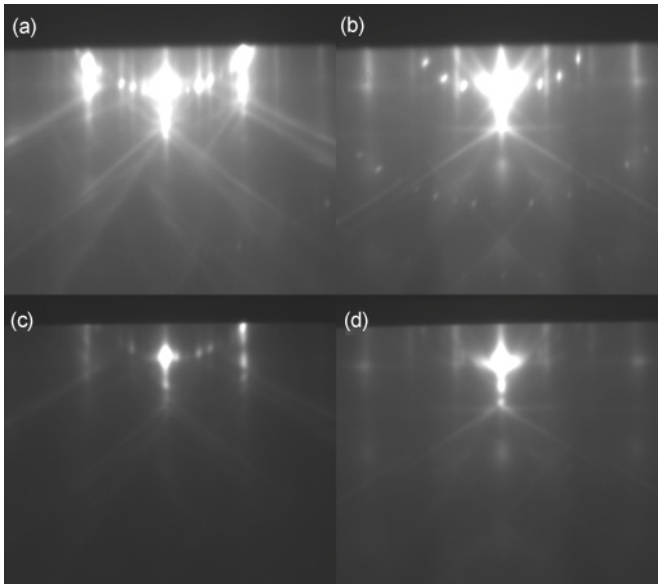

FIG. 7. RHEED pattern of Si(111) covered by 0.6 ML B obtained in (a) ⟨112⟩ and (b) ⟨110⟩ azimuth and covered by 1.3 ML in (c) ⟨112⟩ and (d) ⟨110⟩ azimuth.

formed by B in S_5 sites should be dependent on both T and annealing duration. In the next set of experiments therefore, the influence of the annealing duration on the surface structure formation was investigated. For that purpose 0.6 ML B were initially deposited at 860 K on Si(111). Afterward the samples were annealed at 1080 and 1130 K (Figs. 8 and 9) for different durations. Annealing at 1080 K for 20 min had no impact on the UPS spectra (Fig. 8). After 40 min a slight shift of the

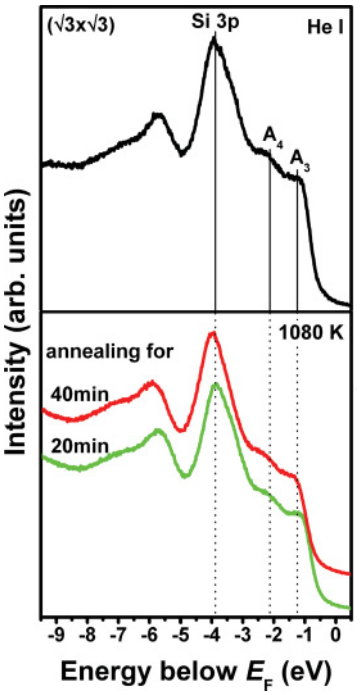

FIG. 8. (Color online) UPS spectra of the initially defect-free Si(111)$(\sqrt{3}\times\sqrt{3})R30^\circ$-B surface ($c_B$ = 0.6 ML) (top) and after subsequent annealing at 1080 K for 20 and 40 min.

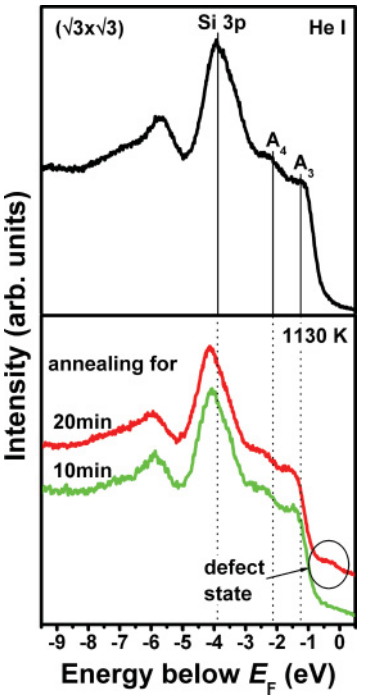

FIG. 9. (Color online) UPS spectra of the initially defect-free Si(111)$(\sqrt{3}\times\sqrt{3})R30^\circ$-B surface ($c_B$ =0.6 ML) (top) and after subsequent annealing at 1130 K for 10 and 20 min.

spectrum by 0.1 eV toward lower energy was observed, which already indicates the formation of surface defects.[20] Annealing at 1130 K already leads after 10 min to a significant shift of about 0.3 eV toward lower energy (Fig. 9) and during further annealing the surface defect state around −0.4 eV becomes clearly visible after 20 min. That clearly demonstrates that the quantity of surface defects is further increased compared to annealing at 1080 K for the same annealing duration, indicating a significant B surface depletion due to B bulk diffusion at 1130 K. However, the state at −2.1 eV is still visible during the different annealing steps, which we attribute to the fact that B clusters do not dissolve completely.

A higher T of 1200 K for significant B bulk diffusion was reported based on XPS investigations of Si(111) covered by B, where B_2O_3 was used as solid source for B evaporation. However, UPS spectra obtained for samples exhibiting $(\sqrt{3}\times\sqrt{3})$ structure after annealing at 1073 K showed the surface defect state corresponding to insufficient B at the surface.[21]

C. UPS study of B surface segregation

The samples in these investigations were prepared by deposition of 0.6 ML B at 860 K and subsequent annealing at 1000 K for 10 min. Under these conditions, Si dangling bonds are not formed and simultaneously B excess can be assumed to be in a more equilibrium-like configuration at the surface. In the first set of experiments, 20 BL Si were grown afterward at 700 K and annealed at various T and duration to initiate B surface segregation. Thereby, annealing was restricted to a maximum T, where even only 4-BL-thick Si layers grown in twin orientation with respect to the underlying substrate are stable against structural reordering into an untwinned

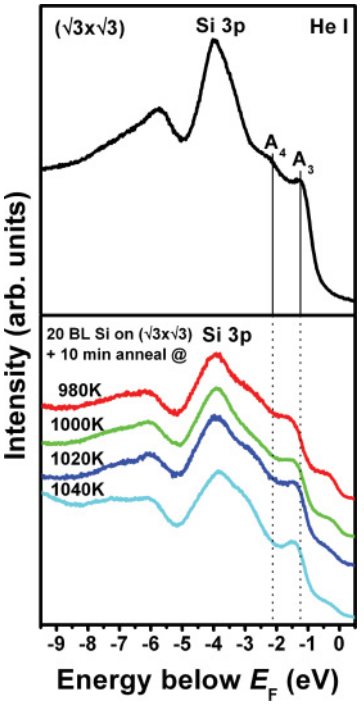

FIG. 10. (Color online) UPS spectra obtained for an initially defect-free Si(111)$(\sqrt{3}\times\sqrt{3})R30^\circ$-B surface ($c_B = 0.6$ ML) (top), and after deposition of 20 BL Si and subsequent annealing for 10 min at different T.

orientation.[47] Otherwise, the interfacial stacking fault, necessary to create artificial structures, would be eliminated.

Accompanying RHEED studies demonstrated that during deposition of some monolayers of Si a change of the surface structure occurred from $(\sqrt{3}\times\sqrt{3})R30^\circ$ to (1×1), as we observed already in earlier studies.[9] After further growth of at least 10 ML Si weak spots appeared in the RHEED pattern corresponding to the (7×7) surface structure. After subsequent annealing the surface structure changed again and the RHEED pattern always exhibited a well-developed B-induced $(\sqrt{3}\times\sqrt{3})R30^\circ$ surface structure, indicating significant B surface segregation.

Figure 10 shows UPS spectra of surfaces prepared by annealing of stacks with 0.6 ML B buried under 20 ML Si at various T for 10 min. First, compared to the initial surface (shown at the top of the figure) the spectra obtained for Si(111)$(\sqrt{3}\times\sqrt{3})R30^\circ$ induced by B segregation do not exhibit the A_4 state appearing at -2.1 eV. Based on our suggestion that that state is associated with B clusters, we can conclude that no B clusters are present at the surface. Therefore, we suggest that segregation of B clusters is excluded under the conditions used. That is supported by earlier studies of B segregation in Si, where the activation energy of B mobilization was attributed to the dissociation of B clusters.[48] In this context, however, we cannot exclude *a priori* that B clusters are still present in the interface, since stable B clusters were found to exist in Si after B implantation and subsequent annealing.[38]

In the spectra it is seen further that the peak located at around -4 eV broadens to the high-energy side and becomes similar to that in Si(111)(7×7), which can be assumed to result from the distribution of a part of the initially deposited 0.6 ML B across the grown layer during annealing.[49–51] This is accompanied by the development of a well-pronounced surface state around -1.5 eV, due to a better ordering of the surface structure, where B at the surface is now only within the subsurface sites. However, a peak related to surface defects is visible at around -0.4 eV indicating that there is not sufficient B accumulated at the surface during annealing for 10 min at T up to 1040 K. This is accompanied by a nearly constant shift of the spectra by 0.3 eV toward the low-energy side, which can be interpreted as a pinning of the Fermi level due to Si dangling bonds, as explained recently.[20] The intensity of the defect state is reduced with an increase in annealing T, i.e., there is more B accumulated into the surface at higher T. This means surface segregation should dominate over B bulk diffusion. That compares well to results recently obtained in RHEED studies, where the growth behavior of Si on Si(111)$(\sqrt{3}\times\sqrt{3})R30^\circ$ was found always to be reproducible for surfaces prepared by surface segregation of buried B.[13] Furthermore, distributions of initial 0.4 ML B buried below 15 nm Si were recently analyzed as a function of the Si growth T using quantitative elastic recoil detection (ERD).[52] The results of the ERD study clearly demonstrated that at T below 1173 K strong surface segregation occurs, whereas nearly all the buried B remains within the interface at $T < 900$ K.

Despite the strong B surface segregation observed also in our studies, it was not clear at this point whether or not a perfect surface structure is attainable during surface segregation. For that reason in the next set of experiments the annealing duration was varied.

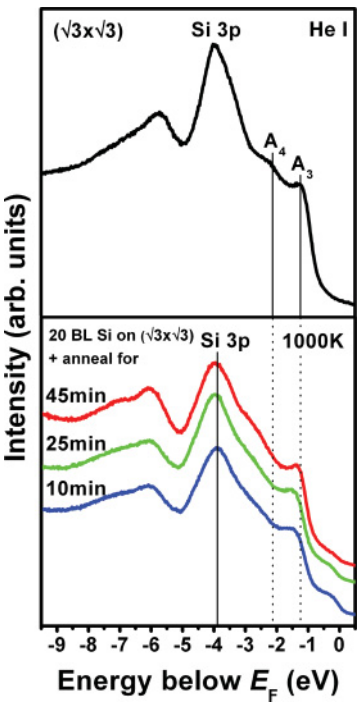

FIG. 11. (Color online) UPS spectra obtained for an initially defect-free Si(111)$(\sqrt{3}\times\sqrt{3})R30^\circ$-B surface after 0.6 ML B deposition at 860 K (top), and after deposition of 20 BL Si at 700 K and subsequent annealing at 1000 K for different durations.

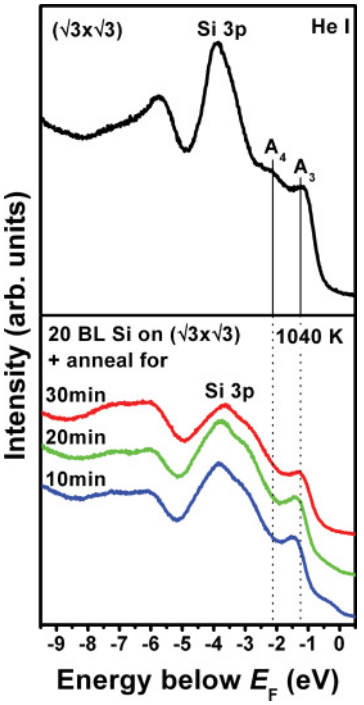

FIG. 12. (Color online) UPS spectra obtained for an initially defect-free Si(111)$(\sqrt{3}\times\sqrt{3})R30^\circ$-B surface after 0.6 ML B deposition at 860 K (top), and after deposition of 20 BL Si at 700 K and subsequent annealing at 1040 K for different durations.

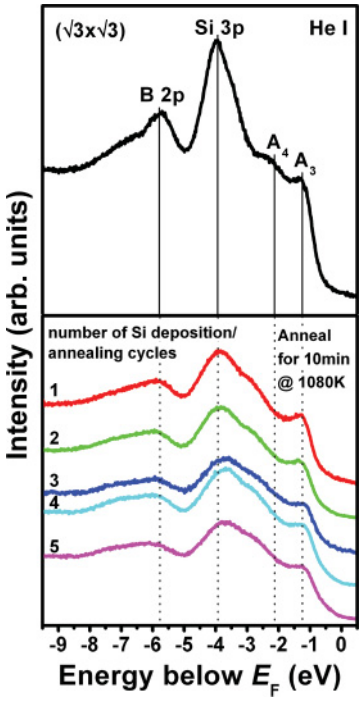

FIG. 13. (Color online) UPS spectra taken for samples after respective deposition/annealing cycles, where each cycle consist of 8 BL Si MBE growth at 700 K and subsequent annealing at 1080 K for 10 min. The spectrum taken for the initial Si(111)$(\sqrt{3}\times\sqrt{3})R30^\circ$-B surface, is also shown (top).

Figures 11 and 12 show UPS spectra obtained for the initial Si(111)$(\sqrt{3}\times\sqrt{3})R30^\circ$-B surface and for samples with 20 BL silicon deposited on the 0.6-ML-B-covered Si(111) surface after annealing at 1000 K (Fig. 11) and 1040 K (Fig. 12) for different durations. After annealing at 1000 K even for 45 min the surface state related to Si dangling bonds is still visible, i.e., Si is in T_4 sites with Si in S_5 directly below. Thus, the thermal activation to stimulate surface migration is still not sufficient to accumulate enough B in the surface, although the observed RHEED pattern showed a well-developed $(\sqrt{3}\times\sqrt{3})$ surface structure. A renewal of the surface structure with no indication of surface defect states was achieved by annealing at 1040 K for 30 min. This indicates that a surface structure without distinct visible surface defect states is achievable via surface segregation for $c_B = 0.6$ ML. The segregation of B at the Si(111)$(\sqrt{3}\times\sqrt{3})R30^\circ$-B surface may be described to be a result of the moving of dopants from high-energy substituted bulk sites to the low-energy subsurface.[53] The surface structure formed in this way exhibits the lowest energy.[15,17,28,50,53]

Finally, surface structure formation by surface segregation was studied during several Si deposition and annealing cycles corresponding to the preparation of artificial Si structures. Each cycle consisted of growth of 8 BL Si at 700 K and subsequent annealing at 1080 K for 10 min, as illustrated in Fig. 2. The growth was started also on an initially defect-free B-covered surface. Before the first and then after each cycle an UPS measurement was performed.

Figure 13 shows the spectra obtained after the respective deposition/annealing cycle together with the spectrum for the initial B-covered Si(111) surface. The spectra for the Si(111)$(\sqrt{3}\times\sqrt{3})R30^\circ$-B surface induced by B surface segregation do not display the state associated with surface defects after at least three cycles without additional B supply. Only after the fourth cycle, which is after the growth of 32 BL, does a small increase in intensity at around -0.5 eV indicate slight B depletion at the surface.

With increasing number of deposition/annealing cycles the spectra shift toward higher energy, whereas no such shift was observed for 20 BL of Si (Figs. 10–12). At this stage, we can only speculate about the reason for that behavior. On the one hand, this could indicate that the surface becomes metallic so that the Fermi level is further shifted into a position where it lies within the valence band.[54] On the other hand, this could also indicate that the top of the valence band somehow is modified because areas of artificially stacked Si structures are formed by periodical creation of interfacial stacking faults along the [111] growth direction at a distance of only a few monolayers apart. In such an artificially stacked Si structure, such as hexagonal Si, the threefold-degenerate valence band of the cubic Si splits into a twofold degenerate and one lower split-off band; thereby the crystal-field splitting increases with the hexagonality.[55,56] That, however, will be a subject of further investigations.

IV. SUMMARY AND CONCLUSIONS

Adsorption of elemental B on Si(111) and subsequent evolution of $(\sqrt{3}\times\sqrt{3})R30^\circ$ surface structure formation was studied using ultraviolet photoelectron spectroscopy as a function of different parameters, such as substrate T during B deposition, B coverage, and annealing T and duration. Furthermore, the surface structure formation induced by surface segregation

of buried B was also studied in detail by deposition of Si on an initially defect-free Si(111)$(\sqrt{3} \times \sqrt{3})R30^\circ$ surface and a subsequent annealing. From the results obtained, the following conclusions can be drawn.

Deposition of 0.6 ML B and annealing in the range $800 < T < 1100$ K on Si(111) results in an effective doping of near-surface regions and in the formation of a $(\sqrt{3} \times \sqrt{3})R30^\circ$ surface superstructure without defects resulting from Si dangling bonds. This clearly indicates that B occupies subsurface sites already at relatively low T. However, in the case of B adsorption at the critical level an additional surface state was observed, which is attributed to electron emission associated with small B clusters present at the surface. The clusters do not dissolve completely even after annealing at $T > 1100$ K. At such high T, however, significant B bulk diffusion sets in, leaving behind Si dangling bonds due to depletion of B at the surface within some surface regions. That indicates an inhomogeneous distribution of B across the surface in the case of B deposition and also demonstrates that the arrangement of B within the surface in the case of deposition is governed by both surface kinetics and thermodynamics.

In contrast, annealing of 0.6 ML B buried below several monolayers of MBE-grown Si at T around 1040 K for several tens of minutes results in a reoccurrence of a defect-free B-induced Si surface structure, even after several deposition and annealing cycles. That demonstrates the dominance of B surface segregation over bulk diffusion. Here, surfaces exhibiting no surface states are attainable.

This clearly indicates that the overall surface structure obtained by deposition of B differs compared to those obtained after B surface segregation. In the case of B deposition we cannot attain a surface nearly free of structural disorder. This is in contrast to the general assumption that independent of the approach (by adsorption from the gas phase or diffusion from the bulk) the equilibrium configuration at the surface should always be the same.

Based on the results of our studies, optimized conditions have been established for the preparation of a defect-free B-induced Si(111)$(\sqrt{3} \times \sqrt{3})R30^\circ$ surface structure during the different steps necessary for the epitaxial growth of artificially stacked Si structures. The application of these conditions should result in a significant improvement of the MBE of such new Si structures. The proof of that statement will be a subject of further work.

ACKNOWLEDGMENT

The authors would like to acknowledge the partial support of the work by the Deutsche Forschungsgemeinschaft (DFG Project No. FI 726/3-2).

[1] L. Zhang, J.-W. Luo, A. Zunger, N. Akopian, V. Zwiller, and J.-C. Harmand, Nano Lett. **10**, 4055 (2010).
[2] R. E. Algra, M. A. Verheijen, M. T. Borgström, L.-F. Feiner, G. Immink, W. J. P. van Enckevort, E. Vlieg, and E. P. A. M. Bakkers, Nature (London) **456**, 369 (2008).
[3] Y. Ohno, N. Yamamoto, K. Shoda, and S. Takeda, Jpn. J. Appl. Phys. **46**, L830 (2007).
[4] A. Fissel, Phys. Rep. **379**, 149 (2003).
[5] L. Gu, Y. Yu, W. Sigle, N. Usami, S. Tsukimoto, J. Maier, Y. Ikuhara, and P. A. van Aken, Appl. Phys. Lett. **97**, 213102 (2010).
[6] F. J. Lopez, E. R. Hemesath, and L. J. Lauhon, Nano Lett. **9**, 2774 (2009).
[7] J. Arbiol, A. F. i Morral, S. Estrade, F. Peiro, B. Kalache, P. R. I. Cabarrocas, and J. R. Morante, J. Appl. Phys. **104**, 064312 (2008).
[8] J. Nakamura and A. Natori, Appl. Phys. Lett. **89**, 053118 (2006).
[9] A. Fissel, E. Bugiel, C. R. Wang, and H. J. Osten, J. Cryst. Growth **290**, 392 (2006).
[10] D. J. Paul, Thin Solid Films **321**, 172 (1998).
[11] R. L. Headrick, B. E. Weir, J. Bevk, B. S. Freer, D. J. Eaglesham, and L. C. Feldman, Phys. Rev. Lett. **65**, 1128 (1990).
[12] H. Hibino and Y. Watanabe, Jpn. J. Appl. Phys. **44**, 358 (2005).
[13] A. Fissel, J. Krügener, and H. J. Osten, Surf. Sci. **603**, 477 (2009).
[14] H. Hirayama, T. Tatsumi, and N. Aizaki, Surf. Sci. **193**, L47 (1988).
[15] R. L. Headrick, I. K. Robinson, E. Vlieg, and L. C. Feldman, Phys. Rev. Lett. **63**, 1253 (1989).
[16] P. Bedrossian, R. D. Meade, K. Mortensen, D. M. Chen, J. A. Golovchenko, and D. Vanderbilt, Phys. Rev. Lett. **63**, 1257 (1989).
[17] I.-W. Lyo, E. Kaxiras, and Ph. Avouris, Phys. Rev. Lett. **63**, 1261 (1989).
[18] Y. Kumagai, R. Mori, K. Ishimoto, K.-H. Park, and H. Hasegawa, Jpn. J. Appl. Phys. **33**, L817 (1994).
[19] Y. Kumagai, K. Ishimoto, R. Mori, and F. Hasegawa, J. Cryst. Growth **150**, 989 (1995).
[20] A. Fissel, J. Krügener, D. Schwendt, and H. J. Osten, Phys. Status Solidi A **207**, 245 (2010).
[21] R. Cao, X. Yang, and P. Pinetta, J. Vac. Sci. Technol. A **11**, 1817 (1993).
[22] K. Higashiyama, S. Yamazaki, H. Ohnuki, and H. Fukutani, Solid State Commun. **87**, 455 (1993).
[23] N. Okasabe, Y. Tanishiro, K. Yagi, and G. Honjo, Surf. Sci. **109**, 353 (1981).
[24] A. V. Latyshev, A. B. Krasilnikov, A. L. Aseev, L. V. Sokolov, and S. I. Stenin, Surf. Sci. **254**, 90 (1991).
[25] G. V. Hansson and R. I. G. Uhrberg, Surf. Sci. Rep. **9**, 197 (1988).
[26] H. J. Lewerenz, Chem. Soc. Rev. **26**, 239 (1997).
[27] R. I. G. Uhrberg, G. V. Hansson, J. M. Nicholls, P. E. S. Persson, and S. A. Flodström, Phys. Rev. B **31**, 3805 (1985).
[28] E. Kaxiras, K. C. Pandey, F. J. Himpsel, and R. M. Tromp, Phys. Rev. B **41**, 1262 (1990).
[29] R. I. G. Uhrberg, R. D. Bringans, M. A. Olmstead, R. Z. Bachrach, and J. E. Northrup, Phys. Rev. B **35**, 3945 (1987).
[30] T. Stimpel, J. Schulze, H. E. Hoster, I. Eisele, and H. Baumgärtner, Appl. Surf. Sci. **162/163**, 384 (2000).
[31] T. Stimpel, H. E. Hoster, J. Schulze, H. Baumgärtner, and I. Eisele, Mater. Sci. Technol. **18**, 721 (2002).
[32] P. J. Chen, M. L. Colaianni, and J.T. Yates Jr., J. Appl. Phys. **72**, 3155 (1992).
[33] F. K. Perkins, R. A. Rosenberg, S. Lee, and P. A. Dowben, J. Appl. Phys. **69**, 4103 (1991).

[34]T. B. Fryberger, J. L. Grant, and P. C. Stair, Langmuir **3**, 1015 (1987).
[35]D. J. Joyner and R. F. Willis, Philos. Mag. A **43**, 815 (1981).
[36]L. Hanley, J. L. Whitten, and S. L. Anderson, J. Phys. Chem. **92**, 5803 (1988).
[37]O. Cojocaru-Miredin, E. Candel, F. Vurpillot, D. Mangelinck, and D. Blavette, Scr. Mater. **60**, 285 (2009).
[38]K. Ohmori, N. Esashi, E. Atoro, D. Sato, H. Kawanishi, Y. Higashiguchi, and Y. Hayafuji, Jpn. J. Appl. Phys. **46**, 14 (2007).
[39]G. Bisognin, D. De Salvador, E. Napolitani, A. Carnera, E. Bruno, S. Mirabella, F. Priolo, and A. Mattoni, Semicond. Sci. Technol. **21**, L41 (2006).
[40]M. Okamoto, K. Kazunobu, and K. Takayanagi, Appl. Phys. Lett. **70**, 978 (1997).
[41]B. Kiran, G. G. Kumar, M. T. Nguyen, A. K. Kandalam, and P. Jena, Inorg. Chem. **48**, 9965 (2009).
[42]H.-J. Zhai, B. Kiran, J. Li, and L.-Sh. Wang, Nature Mater. **2**, 827 (2003).
[43]H. Kawanowa, R. Souda, K. Yamamoto, S. Otani, and Y. Gotoh, Phys. Rev. B **60**, 2855 (1999).
[44]H. Kawanowa, K. Yamamoto, S. Otani, K. Kobayashi, Y. Gotoh, and R. Souda, Surf. Sci. **463**, 191 (2000).
[45]H.-J. Zhai, L.-Sh. Wang, A. N. Alexandrova, and A. I. Boldyrev, J. Chem. Phys. **117**, 7917 (2002).
[46]B. Kiran, S. Bulusu, H.-J. Zhai, S. Yoo, X. Ch. Zeng, and L.-Sh. Wang, Proc. Natl. Acad. Sci. USA**102**, 961 (2005).
[47]H. Hibino and T. Ogino, Surf. Rev. Lett. **7**, 631 (2000).
[48]A. Yu. Kuznetsov, P. Leveque, A. Hallen, B. G. Svensson, and A. N. Larsen, Mater. Sci. Semicond. Process. **3**, 279 (2000).
[49]W. Eberhardt, G. Kalkoffen, C. Kunz, D. Aspnes, and M. Cardona, Phys. Stat. Sol. (b) **88**, 135 (1978).
[50]H. Q. Shi, M. W. Radny, and P. V. Smith, Surf. Rev. Lett. **10**, 201 (2003).
[51]F. J. Himpsel, G. Hollinger, and R. A. Pollak, Phys. Rev. B **28**, 7014 (1983).
[52]J. Schulze, H. Baumgärtner, C. Fink, G. Dollinger, I. Gentchev, L. Görgens, W. Hansch, H. E. Hoster, T. H. Metzger, R. Paniago, T. Stimpel, T. Sulima, and I. Eisele, Thin Solid Films **369**, 10 (2000).
[53]V. G. Zavodinsky, I. A. Kuyanov, and E. N. Chukurov, J. Vac. Sci. Technol. A **17**, 2709 (1999).
[54]J. E. Rowe, G. K. Wertheim, and D. M. Riffe, J. Vac. Sci. Technol. A **9**, 1020 (1991).
[55]C. Raffy, J. Furthmüller, and F. Bechstedt, Phys. Rev. B **66**, 075201 (2002).
[56]M. Murayama and T. Nakayama, J. Phys. Soc. Jpn. **61**, 2419 (1992).